ELSEVIER

Journal of Chromatography A, 971 (2002) 73–86

JOURNAL OF CHROMATOGRAPHY A

www.elsevier.com/locate/chroma

DNA-induced inter-particle cross-linking during expanded bed adsorption chromatography
Impact on future support design

Irini Theodossiou[1], Owen R.T. Thomas*

Center for Process Biotechnology, BioCentrum-DTU, Technical University of Denmark, Building 223, Søltofts Plads, DK-2800 Lyngby, Denmark

Received 26 October 2001; received in revised form 7 June 2002; accepted 7 June 2002

Abstract

We have investigated the effects of adsorbent size, ionic capacity and surface immobilised polymers on dynamic capacity and changes occurring to beds of anion-exchangers during the binding of DNA. During application of low concentrations of ''3–20 kilobase'' calf thymus DNA feeds to expanded beds of anion-exchangers, the bed heights dropped progressively as DNA molecules physically cross-linked neighbouring adsorbent particles together, to form severely aggregated fluidised beds. In plots of dynamic binding capacities and absolute changes in bed porosity at maximum contraction, against the inverse of the mean hydrated particle radii, the anion-exchangers were observed to split into three distinct, but different clusters in each case. The highest index of surface packing of DNA was observed for two prototype pellicular supports, one derivatised with highly charged high molecular mass polyethyleneimine (M_r~50 000) and the other with long dextran (M_r~500 000) chains weakly derivatised with DEAE. However, the ability of the surfaces of these two matrices to bring about bed contraction, was strikingly different. The highly charged surface afforded by coupling of polyethyleneimine exhibited a three-fold higher tendency to interact with neighbouring particles in the presence of DNA than that of the dextran DEAE support. The implications of these findings on the design of future expanded bed materials for separation of both proteins and nucleic acids are discussed.

Keywords: Expanded bed adsorption; Support design; Stationary phases, LC; Adsorption; Anion-exchangers; Fluidised bed chromatography; DNA

1. Introduction

Many manufacturers of new biotech products are looking for ways to make their manufacturing processes more cost-effective, and for those produced by fermentation the key to achieving this goal may be to streamline downstream processing operations, which can account for a very large percentage of the total production costs [1,2]. Purification schemes comprising multiple operations, although very common in the biopharmaceutical industries, result in excessive product losses combined with high capital

*Corresponding author. Tel.: +45-45-252-703; fax: +45-45-884-148.

E-mail address: ot@biocentrum.dtu.dk (O.R.T. Thomas).

[1]Present address: Alpharma ApS, Dalslandsgade 11, P.O. Box 1736, DK-2300 Copenhagen, Denmark.

0021-9673/02/$ – see front matter
PII: S0021-9673(02)00820-8

and labour costs. In recent years this situation has driven a growing interest in the design and application of robust techniques for capturing target products directly from crude particle-containing process liquors [3–7]. Such capture techniques eliminate the need for extensive feedstock conditioning (principally clarification), thus contributing to a cheaper faster process, delivering higher bioproduct yield. Currently, perhaps the most promising and practical of these is expanded bed adsorption (EBA), which is a successful hybrid of conventional packed and fluidised beds [4,6,8,9]. In EBA, dense adsorbent particles of a defined size distribution are fluidised by a mobile phase directed upwards to form a stable ''classified'' fluidised bed, which is commonly termed an ''expanded bed'' [4,6]. Key to the performance of the EBA system is that axial mixing is very low and that the void fraction is increased to permit the application of crude bioprocess liquors, such as fermentation broths or cell homogenates, without the risk of blocking the bed. Under ideal conditions, where the correct flow regime is used and particle–particle aggregation is absent, the chromatographic behaviour of an expanded bed approximates to that of a packed bed system. Despite initial successes [10,11], however, the technique is currently not sufficiently robust to encourage widespread industrial application [7].

The current weaknesses of EBA systems mainly revolve around fouling by solids and other components (especially large colloidal molecules) present in crude biological suspensions. A potential limitation of any porous adsorbent is a propensity to become ''plugged'' with biological foulants and the difficulty in removing such substances [12,13]. However, in EBA a much greater problem is caused by the physical cross-linking of neighbouring adsorbent particles by biomass or large colloidal molecules (especially nucleic acids), which can lead to gross breakdown of the structure of the expanded bed and consequent loss of chromatographic performance [6,14–20]. Commercially available EBA adsorbents are direct descendants of packed bed chromatography matrices (which have been designed for the purification of proteins) and in order to form a stable, stratified bed at reasonable linear processing velocities, current materials have large particle diameters, wide size distribution (ratio of the largest and smallest particle >2.2) and high specific density [6]. However, a number of authors [5,6] have suggested that in order to increase sorption performance, further improvements in matrix design should concentrate on the development of particles with enhanced mass transport capability, and that one possible way to achieve this would be to manufacture smaller adsorbent beads with increased density. In recent work we introduced small, high-density pellicular expanded bed adsorbents, possessing massively enhanced binding capacities for ''nanoparticulate'' molecules, such as plasmid DNA [18–21]. In ''clean'' systems [21,22] these supports exhibit lower axial dispersion and improved resolution (lower height equivalent to a theoretical plate, HETP) over their commercial counterparts; properties, which encourage the use of low settled bed heights and even permit the employment of linear gradient elution protocols [20]. However, despite many desirable features, we have identified a potentially serious problem affecting the use of expanded bed adsorbents of small particle size in complex process environments; namely an increased tendency for inter-particle cross-linking to occur in the presence of problem species, such as cells, cell debris or nucleic acids [19–21].

This paper describes the interaction of calf thymus DNA with anion-exchange adsorbents in expanded beds. By using various supports (commercial and pellicular prototypes) and binding conditions, we show how particle diameter, surface features and surface chemistry influence both DNA binding capacity and DNA induced inter-particle cross-linking. The implications of our findings on the future design of robust expanded bed adsorbents for separation of nucleic acids and proteins is discussed.

2. Materials and methods

2.1. Materials

Streamline DEAE, Streamline QXL and Q Sepharose FF were all purchased from Amersham Biosciences (Uppsala, Sweden). The UFC DEAE, UFC polyethyleneimine (PEI) and various types and lots of stainless steel cored prototype (see Table 1) expanded bed adsorbents [21] were manufactured

Table 1
Characteristics of expanded bed supports used in this study (see Section 2.2 for details)

Number code	Support	Ligand	Particle size distribution; mean (μm)	Bulk density[a] (g ml^{-1})	Particle density[a] (g ml^{-1})	% (v/v) core content[a,b]	Bulk ionic capacity[c] (mmol Cl$^-$ ml^{-1})	Normalised ionic capacity[d] (mmol Cl$^-$ ml^{-1})
Commercial								
2	Streamline	DEAE	65–300; 143	1.09±0.01	1.15±0.02	22.54±0.40	0.14	0.181
3	Streamline	QXL	65–260; 143	1.09±0.01	1.15±0.02	31.06±0.91	0.22	0.319
4	UFC	DEAE	105–300; 198	1.22±0.02	1.37±0.03	57.28±0.39	0.058	0.136
5	UFC	PEI	105–300; 175	1.30±0.02	1.50±0.03	67.42±0.60	0.026	0.080
Prototypes								
UFC "40–100"								
6	62258J	DEAE	49–104; 73.6	2.0±0.06	2.67±0.10	47.80±0.99	0.031	0.059
UFC "20–40"								
1	61374J	no ligand	27–50; 38.1	2.72	3.87	56.50	0.001	0.002
7	61409J	DEAE	25–48; 33.4	3.00	4.33	63.39	0.022	0.067
8	61589J	PEI 2000[e]	27–50; 34.3	3.06±0.35	4.48±0.59	64.38±4.26	0.024	0.040
9	61588J	PEI 25 000[e]	27–48; 34.6	3.35±0.09	4.91±0.15	67.76±1.18	0.013	0.086
10	61474J	PEI 50 000[e]	17–50; 34.8	2.89±0.13	4.15±0.21	60.35±1.22	0.034	0.096
11	61635J	DEAE dextran	25–48; 32.3	3.20	4.67	64.78	0.067	0.179

[a] Some values are from duplicate or triplicate measurements and these are given as the mean±SD (σ_{n-1}).
[b] The volumetric core contents were derived from dry mass measurements and assuming density values of: 2.5 g ml^{-1} for the quartz and glass [23] core materials used in commercial Streamline and UFC adsorbents, respectively; 7.8 g ml^{-1} for the steel cores of the prototype supports; 1.02 and 1.1 g ml^{-1} for wet and dry agarose, respectively. In our calculations we have assumed mass contributions from dextran, PEI and ligands as being negligible.
[c] Measured bulk ionic capacities.
[d] Normalised ionic capacities were obtained from bulk values after accounting for the volumes occupied by the inert core materials.
[e] The numbers refer to the mean M_r of the PEI employed.

and supplied by UpFront Chromatography A/S (Copenhagen, Denmark). The stainless steel metal powder (Anval 316L Code 5513; 22–44 μm gas atomised spherical particles with a density of 7.8 g ml^{-1}) was received as a gift from Dynamet Anval (Torshälla, Sweden). The materials, ammonium iron(III) sulphate dodecahydrate, mercuric thiocyanate and deoxyribonucleic acid from calf thymus (type I: sodium salt "highly polymerised") were obtained from Sigma–Aldrich (St Louis, MO, USA) as were all other chemicals used in this study.

2.2. Support characterisation

All expanded bed matrices were examined with a Nikon Optiphot 2 microscope (Nikon, Melville, NY, USA) fitted with a Kappa CF−8/1 FMC monochrome video camera (Kappa Opto−electronics, Gleichen, Germany) and digitised micrographs and particle size distributions were produced with the aid of the Image−Pro Plus software (version 4.1 for Windows; Media Cybernetics, Silver Spring, MD, USA) program.

The bulk densities of supports were determined simply from weighing known settled volumes (0.5 or 1 ml) of each matrix. Estimates of particle density were obtained from the same measurements by assuming a sample voidage of 0.4 [24] in all cases. The determination of the content of densifying core elements (i.e. stainless steel, glass or quartz fillers) in all expanded bed adsorbent preparations was determined in the following way. Supor membrane disc filters (0.45 μm hydrophilic polyether sulphone, Pall Gelman Labs, Ann Arbor, MI, USA) were dried in a microwave for 10 min at a power setting of 150 W and then weighed. Known settled volumes (0.5 or 1 ml) of supports were transferred onto the pre-dried and pre-weighed filter discs and then desiccated at 106 °C over 72 h (to constant mass) before recording their dry masses. Parallel dry mass measurements of Q Sepharose FF, a packed bed anion-exchange adsorbent composed entirely of cross-linked agarose,

and of a spherical ''22–44 μm'' 316L stainless steel powder used to manufacture the steel cored prototype expanded bed matrices were also performed. The former allowed an estimate of the dry density of agarose to be calculated, while the latter served as a control to compensate for slight changes in mass due to thermal oxidation of the stainless steel cores of prototype adsorbents.

The methods used to determine the total ionic capacity of the supports used in this study, were taken from Pitfield [25]. Various amounts (0.5 to 2 ml settled volume) of anion-exchangers were incubated with 50 ml of 2 *M* NaCl for 1.5 h to convert them into the hydrochloride salt or quaternary alkyl ammonium chloride form. Excess acid was then removed from the supports by washing three times on a glass sinter with 50 ml aliquots of Milli-Q water, before transferring the drained materials to plastic 100 ml bottles containing 50 ml of 0.1 *M* NaOH and mixing at 150 rpm for 24 h on an orbital shaker (Infors, Basel, Switzerland). In this step the excess base (OH^-) displaces the Cl^- ions from the supports [26], and following settling of the latter, 1 ml fractions of the liquid phases were assayed for chloride ion content using the colorimetric method described by Vogel [27] involving mercury(II) thiocyanate. In the assay the displacement of the thiocyanate ion from mercury(II) thiocyanate by Cl^- in the presence of ferric ions results in the formation of a highly coloured iron(III) thiocyanate complex and the intensity of its colour is proportional to the original chloride ion concentration. This assay was performed in the following way. A standard curve of chloride ion concentration in the range 0.1 to 2 m*M* was constructed by serial dilution of a 10 m*M* NaCl stock solution (Milli-Q water served as both diluent and blank). In 1.5 ml plastic screw-capped vials, 1 ml aliquots of test samples, standards and blanks were each mixed with 100 μl of 0.25 *M* ammonium iron(III) sulphate in 9 *M* HNO_3 and 100 μl of a saturated solution of mercury(II) thiocyanate in 96% ethanol. Following vigorous mixing on a Vortex-Genie 2 vibrax shaker (Scientific Industries, Bohemia, NY, USA) and 10 min at room temperature, the chloride ion contents in the liquid phases were determined from absorbance measurements at 460 nm conducted in a Lambda 20 UV–Vis spectrophotometer (Perkin-Elmer Analytical Instruments, Shelton, CT, USA).

2.3. Preparation of DNA feedstocks for EBA

Calf thymus DNA was dissolved overnight in 50 m*M* Tris–HCl, pH 8 buffer to a final concentration of 2 mg ml^{-1}, then sonicated on ice (MSE soniprep 150, MSE Scientific Instruments, Sussex, UK), aliquoted into sterile tubes and stored at −20 °C until required. The resulting DNA stock solution was analysed by electrophoresis in a horizontal 0.8% (w/v) ethidium bromide-stained agarose gel and gave a smear running almost the full length of λ*Hin*dIII markers, i.e. from 23 130 to 2 027 base pairs (bp). Feedstocks for expanded bed adsorption studies were prepared by 100-fold dilution of the ''3–20 kilo base pairs (kb)'' DNA stock solution with an appropriate equilibration buffer (50 m*M* Tris–HCl, pH 8 or 0.8 *M* potassium acetate, 10 m*M* EDTA, pH 5.5), to give a final DNA concentration of 20 μg ml^{-1}.

2.4. Expanded bed adsorption chromatography

All expanded bed chromatography experiments were performed on a low pressure GradiFrac chromatography system comprising a HiLoad Pump P-50, on-line conductivity and UV monitors, an in-built fraction collector and a REC102 chart recorder (Amersham Biosciences, Uppsala, Sweden). Given the limiting quantities of stainless steel-cored prototype expanded bed supports made available to us, small 1 cm diameter expanded bed contactors (FastLine10, UpFront Chromatography A/S, Copenhagen, Denmark) were used. The FastLine10 contactor does not permit flow reversal and elution in packed bed mode. Thus, at all stages the columns were operated in expanded mode, using a superficial fluid velocity of 200 cm h^{-1}. Settled beds (~4.5 ml volume) of anion-exchange matrices were expanded with deionised water and washed copiously, before equilibrating with the appropriate binding buffer (i.e. either 50 m*M* Tris–HCl, pH 8 or 0.8 *M* potassium acetate, 10 m*M* EDTA, pH 5.5) until the conductivity of the liquid exiting the column reached that of the incoming equilibration buffer. The expanded bed height, *H*, was then recorded and the flow was stopped for 0.5 h to allow accurate measurement of the initial settled bed height, H_o, of the equilibrated matrix. The beds were then re-expanded with the appropriate binding buffer and once stable expansion

was achieved, DNA (20 μg ml^{-1}) feedstocks prepared as described above were fed to the columns. Liquid exiting the columns was monitored continuously for DNA content by on-line measurement of UV absorbance at 254 nm. In all cases loading of DNA was continued until the column outlet concentration reached at least 20% of the inlet value. The DNA concentration in the feedstock and in collected fractions was determined by absorbance measurements at 260 nm using a spectrophotometer (Lambda 20 UV–Vis; Perkin-Elmer). In all experiments the bed height was periodically recorded and visual observations of bed behaviour were carefully documented with the aid of a hand-held magnifying glass and a digital camera. All of the features observed and schematically represented in Fig. 2 were clearly visible to the naked eye.

3. Results and discussion

3.1. Support characterisation

All of the expanded bed materials employed in this work are agarose-based composites comprising quartz, glass or stainless steel elements to provide the necessary density. Expanded bed supports commercially available from UpFront Chromatography are prepared by coating non-porous glass spheres with agarose (Fig. 1) to give spherical materials with particle density and size ranges of 1.4–1.6 g ml^{-1} and 100–300 μm, respectively [28]. The Streamline anion-exchangers from Amersham Biosciences (Uppsala, Sweden) are described as agarose–quartz composites of lower particle density (~1.2 g ml^{-1}), but very similar size and shape. However, unlike the UFC adsorbent, the densifying element is in the form of small grains evenly distributed throughout the beads (see Fig. 1).

The prototype 40–100 μm and 20–40 μm supports used in this work contain spherical 316L corrosion resistant stainless steel particles as the densifying element and were prepared for us by UpFront Chromatography using proprietary methods [21]. In brief, this involves coating the stainless steel powder (measuring 14–44 μm in our analysis, Fig. 1), with 6% agarose and after washing, successive sieving through 100 and 40 μm meshes yields ''40–100'' and ''20–40'' μm fractions, which are then strengthened by cross-linking with epichlorohydrin. Most of the beads in ''20–40'' μm preparations (Fig. 1) comprise single particle cores thinly encased in agarose (average depth of ~5 μm) and are roughly spherical; but a subset (8–46% of the population depending on the preparation) of elliptical bi-cored species are also present. In contrast, nearly all of the beads in the ''40–100'' μm preparation (Fig. 1) are multi-cored and spherical (~5% deviate from a sphere). Significant batch-to-batch variations in particle size and density for ''20–40'' μm supports (see Table 1) stem from difficulties in achieving precise control over the agarose coating step. For a ''100–300'' μm preparation, a few micrometres variation in depth of the agarose layer will have very little impact on the general bed expansion characteristics or sorption performance, but for a support of very small dimensions 20–40 μm containing a very dense core material, much larger differences in these parameters are to be expected. Thus direct comparison of the performance of differently derivatised preparations of 20–40 μm anion-exchangers is difficult, unless all materials are derived from a common primary particle preparation. Therefore, in order to correlate DNA binding and bed contraction behaviour of the different supports used in this study (see Table 1), all of the materials were individually characterised with respect to appearance, size distribution, bulk and particle densities, volumetric core content and ionic capacity. For ease of identification and cross-referencing each support preparation in this study is given a simple number code (listed in Table 1). Normalised ionic capacity values for the EBA supports were calculated by accounting for the volume occupied by the densifying core elements; the assumption being that Cl^- content determined in the assays arises solely from the anion-exchange capacity of the derivatised agarose gels and not from that of the core materials. Control measurements with the 316L stainless steel particles and preparation 1 (an underivatised UFC ''20–40 μm'' prototype with a normalised ionic capacity of 0.002 mmol Cl^- ml^{-1}) confirmed that anion-exchange contributions from the cores could be neglected.

3.2. General observations on behaviour of expanded beds during DNA binding

Observations drawn from more than 50 dynamic

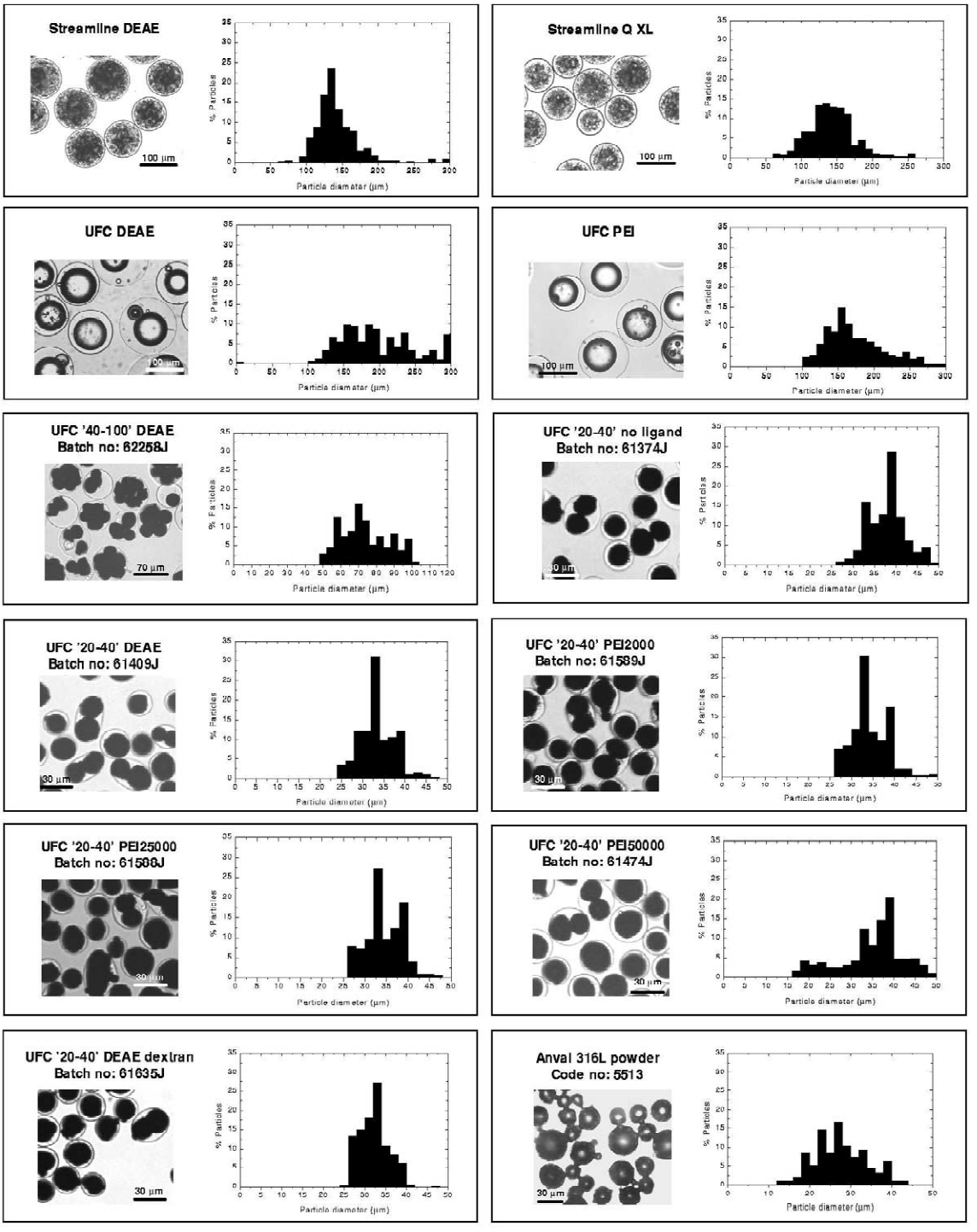

Fig. 1. Light micrographs and particle size distribution plots for the expanded bed materials employed in this study (Table 1). For size distributions, between 260 and 460 particles were counted.

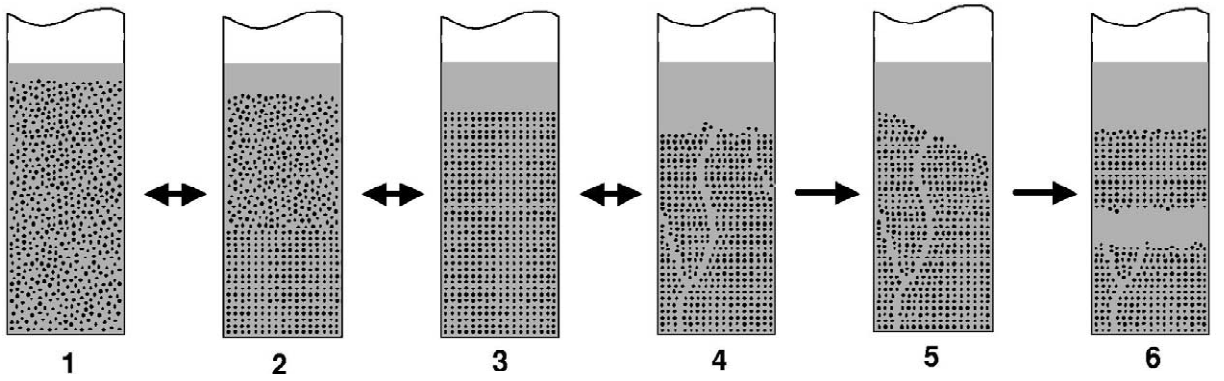

Fig. 2. Schematic illustrations of bed behaviour during application of calf thymus DNA to expanded beds of anion-exchangers. 1—no cross-linking; 2—cross-linking from the column bottom; 3—particle movement frozen; 4—cracks and channels appear in bed; 5—top surface of bed becomes uneven; 6—bed breaks into two or more parts. The arrows indicate reversible (↔) and irreversible (→) transitions.

binding experiments conducted with feedstocks containing low concentrations of DNA and a wide array of anion-exchange supports (Table 1) under different binding conditions are briefly summarised in Fig. 2 and Table 2. Fig. 2 charts the various states (depending on the support and buffer combination under test) that a bed can progress through during continuous application of DNA feed stocks to expanded beds of anion-exchangers. A perfectly fluidised bed (1) starts to cross-link from the bottom (2) until it is completely ''locked'' or ''frozen'' (3). Then cracks and channels appear in the matrix (4). Transitions between states 1–4 are reversible, but should the top surface of the bed cease to be horizontal (5) then irreversible break-up of the bed (6) into two or more parts (which, in contactors of small diameter, rise as solid blocks towards the column exit) is inevitable. Fig. 3a shows breakthrough profiles for the binding of calf thymus DNA to supports in a high ionic strength (59 mS cm^{-1}) potassium acetate buffer. A common feature during the application of DNA containing feedstocks onto expanded beds of anion-exchange supports is to varying extents, depending on the support in question and the ionic strength

Table 2
Observations during the application of calf thymus DNA to expanded beds of anion-exchangers (see Fig. 2)

Support	Buffer	
	50 m*M* Tris–HCl, pH 8 (2.3 mS cm^{-1})	0.8 *M* potassium acetate 10 m*M* EDTA, pH 5.5 (59 mS cm^{-1})
Streamline DEAE (100–300 μm)	2	1–2
Streamline QXL (100–300 μm)	6	2
UFC DEAE (100–300 μm)	2	1–2
UFC PEI (100–300 μm)	6	2–3
UFC DEAE (40–100 μm)	3–4	1–2
UFC no ligand (20–40 μm)	1	1
UFC DEAE (20–40 μm)	4	3
UFC PEI 2000 (20–40 μm)	6	4
UFC PEI 25 000 (20–40 μm)	6	4
UFC PEI 50 000 (20–40 μm)	6	4
UFC DEAE dextran (20–40 μm)	4	2–3

1—no cross-linking; 2—cross-linking from the column bottom; 3—particle movement frozen; 4—cracks and channels appear in bed; 5—top surface of bed becomes uneven; 6—bed breaks into two or more parts.

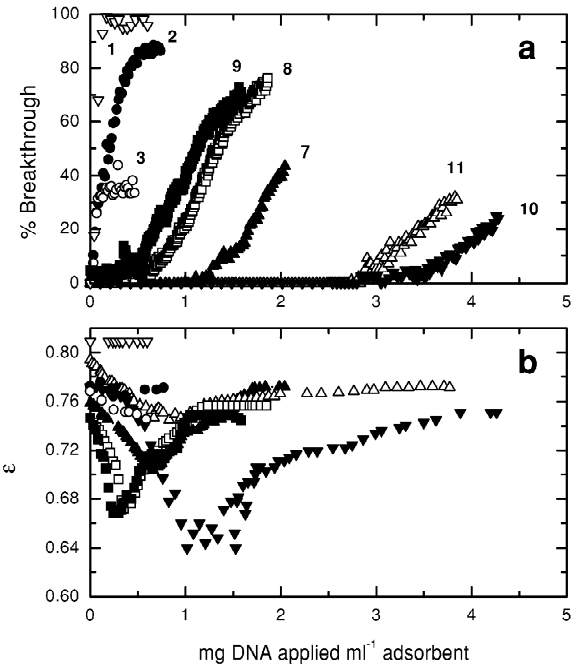

Fig. 3. (a) Breakthrough curves and (b) bed contraction profiles during binding of calf thymus DNA to selected anion-exchange expanded bed adsorbents. Feedstock applied: ~20 μg ml^{-1} sonicated calf thymus DNA in 0.8 *M* potassium acetate, 10 m*M* EDTA, pH 5.5 buffer (conductivity of 59 mS cm^{-1}). 1—UFC ''20–40'' no ligand (ϵ_i=0.80); 2—Streamline DEAE (ϵ_i=0.77); 3—Streamline QXL (ϵ_i=0.77); 7—UFC ''20–40'' DEAE (ϵ_i=0.76); 8—UFC ''20–40'' PEI 2000 (ϵ_i=0.75); 9—UFC ''20–40'' PEI 25 000 (ϵ_i=0.75); 10—UFC ''20–40'' PEI 50 000 (ϵ_i=0.77); 11—UFC ''20–40'' DEAE dextran (ϵ_i=0.80). Bed voidage, ϵ, was calculated using a value of 0.4 for the settled bed [24]. Thus initial porosities (ϵ_i) of expanded beds between 0.75 and 0.80 corresponded to initial H/H_o of 2.4–2.9. Breakthrough data for supports 7 and 10 come from Ref. [19].

employed (see Table 2 and Figs. 2 and 3b), the progressive contraction of the bed caused by DNA molecules ''pulling'' (or flocculating) neighbouring support particles together to produce severely aggregated and physically cross-linked fluidised beds [18–20]. In relatively high ionic strength solutions, this DNA induced contraction process continues until a minimum expanded bed height is reached and shortly thereafter DNA starts to breakthrough and the bed gradually re-expands. Examination of Table 2 illustrates that feedstocks containing low levels of DNA will present significant problems for anion-exchange EBA based separations and that these will be aggravated by: (i) low ionic strength buffers; (ii) supports featuring highly charged hairy surfaces; and (iii) small adsorbent particles.

It has not escaped our attention that the V-shaped profiles in Fig. 3b bear striking resemblance to dosage curves characteristic of stoichiometric flocculation reactions between strong and oppositely charged polymer/particle systems, e.g., flocculation of nucleic acids or cell debris by a strong cationic polymer such as PEI [29,30]. In common with flocculation processes, we observe here (Table 2, Figs. 2 and 3b), and in previous work [18,19], that bed contraction behaviour is dependent on the physical properties, i.e., charge density and molecular size, of the interacting species, namely DNA and the adsorbent surfaces, and the properties of the suspending phase (e.g., pH, ionic strength). Variation in ionic strength and pH will influence the precise aggregation mechanism, i.e., degree of irreversibility and the balance of charge neutralisation–electrostatic patch and polymer bridging contributions [29,30]. In view of the above it is tempting to speculate that the point at which a well-defined minimum bed voidage is reached could correspond to a state where the size of DNA cross-linked adsorbent aggregates reaches a maximum and where the net surface charge they carry is approximately zero. With further application of DNA to the beds it is conceivable that competition for positively charged patches on the surfaces of adsorbents, leading to molecular rearrangement and progressive reduction in the extent of inter-particle bridging, could occur. In the event of this, electrostatic repulsion between neighbouring particle surfaces would be expected to grow and with it progressive dissolution of the particle aggregates accompanied by gradual re-expansion of the bed.

3.3. Correlations between bed contraction and binding capacity

In previous work, it has been have demonstrated that due to its size DNA is unable to access the interior of porous anion-exchange adsorbents and consequently DNA binding occurs only at their exterior surfaces [19,31]. From this it follows that DNA induced particle–particle cross-linking must also be mediated through interactions with the external surface of anion-exchange adsorbent par-

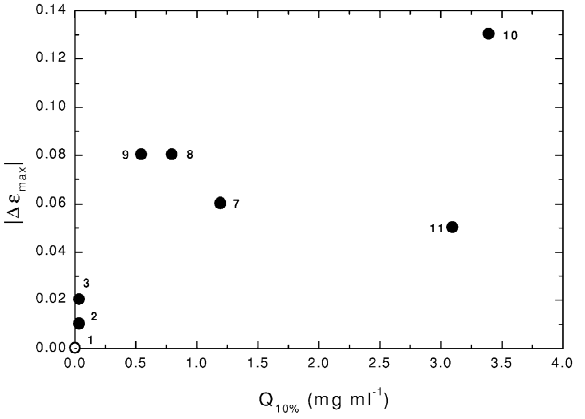

Fig. 4. Absolute change in bed porosity at maximum contraction, $|\Delta\epsilon_{max}|$, versus dynamic DNA binding capacity at 10% breakthrough ($Q_{10\%}$). Feedstock applied: ~20 μg ml^{-1} sonicated calf thymus DNA in 0.8 *M* potassium acetate, 10 m*M* EDTA, pH 5.5 buffer (conductivity of 59 mS cm^{-1}). 1—UFC ''20–40'' no ligand (ϵ_i=0.80); 2—Streamline DEAE (ϵ_i=0.77); 3—Streamline QXL (ϵ_i=0.77); 7—UFC ''20–40'' DEAE (ϵ_i=0.76); 8—UFC ''20–40'' PEI 2000 (ϵ_i=0.75); 9—UFC ''20–40'' PEI 25 000 (ϵ_i=0.75); 10—UFC ''20–40'' PEI 50 000 (ϵ_i=0.77); 11—UFC ''20–40'' DEAE dextran (ϵ_i=0.80).

ticles. Fig. 4 attempts to directly correlate an absolute change in bed porosity at maximum contraction, $|\Delta\epsilon_{max}|$, with the dynamic DNA binding capacity of different anion-exchange expanded bed supports exhibiting very similar initial bed voidages (ϵ_i of 0.75–0.8) under identical operating conditions. Although a general trend towards increasing contraction is observed as the DNA binding capacity (a probe for external surface area) of the support is raised, any direct relationship is somewhat obscured by varying contributions from the range of different ion-exchange groups, charge density and surface features present on the supports tested. We have previously shown that the plasmid and DNA binding capacities of conventional agarose-based packed bed supports are inversely related to particle size, and further, that the grafting or coupling of tentacle-like features (e.g., flexible chains of acrylamide co-polymers or dextran) carrying anion-exchange groups (e.g. DMAE, Q) or performed cationic polymers (e.g., PEI) on to such base materials is a simple and effective way to deliver several fold increases in binding capacity [19,20]. Fig. 5a presents dynamic DNA binding capacities ($Q_{10\%}$) of different EBA supports plotted against the inverse of their mean hydrated particle radii (*r*), whereas Fig. 5b shows the Q_r values derived from Fig. 5a as a function of normalised ionic capacities for the EBA anion-exchangers. The Q_r value for an adsorbent is a rough index of the effectiveness of surface in binding DNA and assumes that the particle is a perfect sphere [18–20]. The functionalised materials are seen to cluster into three groups. The first set exhibit Q_r numbers of ~0.5 μg cm^{-2} and comprise the commercial ''100–300'' μm anion-exchange supports and the DEAE-linked ''40–100'' μm multi-cored

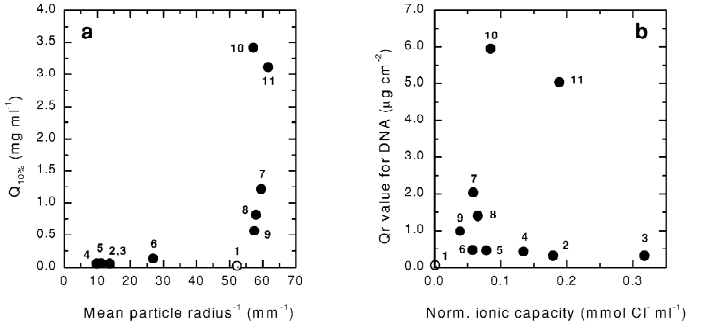

Fig. 5. (a) Dynamic DNA binding capacity at 10% breakthrough ($Q_{10\%}$) as a function of particle radius; and (b) Q_r as a function of normalised ionic capacity during binding of DNA to expanded beds of anion-exchange adsorbents. Q_r is a rough index of the effectiveness of the surface of a spherical adsorbent particle in binding DNA. The Q_r numbers were calculated from the $Q_{10\%}$ data presented in Fig. 5a and mean particle radii derived from Table 1. Feedstock applied: ~20 μg ml^{-1} sonicated calf thymus DNA in 0.8 *M* potassium acetate, 10 m*M* EDTA, pH 5.5 buffer (conductivity of 59 mS cm^{-1}). 1—UFC ''20–40'' no ligand; 2—Streamline DEAE; 3—Streamline QXL; 4—UFC DEAE; 5—UFC PEI; 6—UFC ''40–100'' DEAE; 7—UFC ''20–40'' DEAE; 8—UFC ''20–40'' PEI 2000; 9—UFC ''20–40'' PEI 25 000; 10—UFC ''20–40'' PEI 50 000; 11—UFC ''20–40'' DEAE dextran.

prototype. Three ''20–40'' μm prototypes (DEAE-linked, PEI 2000 and PEI 25 000) make up the second cluster possessing Q_r values between 1 and 2 μg cm^{-2}, while two more ''20–40'' μm prototypes (DEAE dextran and PEI 50 000) with much higher Q_r (>5 μg cm^{-2}) make up the third set. These prototype ''20–40'' μm adsorbents (sets 2 and 3) possess, regardless of surface ligand or charge density, binding capacities that are much higher than expected from simple size reduction of the ''100–300'' μm commercial adsorbents. As stated above, this assumes that their shape approximates to that of a perfect sphere (which is the case for the ''40–100'' and ''100–300'' micrometre-sized supports; see Fig. 1), but inspection under the light microscope (Fig. 1) reveals that many particles within the ''20–40'' μm preparations deviate from this shape and this is especially true for multi-cored (mostly bi-cored) beads, which are ovoid. Furthermore, although not visible under the light microscope, it is plausible that the exterior of these adsorbents is more folded than their larger counterparts, given that the surface of the steel core particles used in their manufacture is not perfectly smooth (this surface irregularity is <0.5 μm; [32]) and is covered by only a very thin layer of agarose (typically ~5 μm c.f. of the order of 20–50 μm for commercial UFC).

Given that bed contraction effects are also mediated through the external surfaces of particles, we have analysed bed contraction data in a similar way to the plots in Fig. 5a and b. Fig. 6a shows the absolute change in bed porosity at maximum contraction $|\Delta\epsilon_{max}|$ for different EBA supports as a function of the inverse of their mean particle radii and in Fig. 6b the individual slope values ($|\Delta\epsilon_{max}|r$) from Fig. 5a are plotted against the normalised ionic capacities for the EBA anion-exchangers. In analogous fashion to Q_r, we envision $|\Delta\epsilon_{max}|r$ as an index of the ability of a given particle's surface to interact with its neighbours via a bridging species, in this case DNA, and again we assume that particle approximates to a perfect sphere. Once more, the anion-exchangers are observed to split into three clusters, but the occupancy of these is very different to those based on Q_r. The first set with $|\Delta\epsilon_{max}|r$ values of 0.7–1.0 μm comprises supports that are exclusively derivatised with the ion-exchanger, DEAE (Streamline DEAE and the 20–40 μm DEAE and DEAE dextran-linked prototypes); the second class ($|\Delta\epsilon_{max}|r$ ~1.4 μm) features Streamline QXL and two ''20–40'' μm prototypes derivatised with low and medium molecular mass PEIs; and the third is the high molecular mass PEI functionalised 20–40 μm support, which exhibits a $|\Delta\epsilon_{max}|r$ value of ~2.3 μm.

3.4. Surface charge and architecture

Initial inspection of Fig. 5b supports an earlier conclusion [19] that surface topography is a much

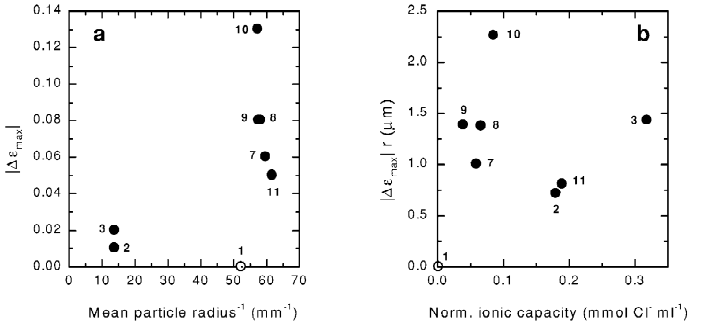

Fig. 6. (a) Absolute change in bed porosity at maximum contraction, $|\Delta\epsilon_{max}|$, as a function of particle radius; and (b) $|\Delta\epsilon_{max}|r$ as a function of normalised ionic capacity during binding of DNA to expanded beds of anion-exchange adsorbents. The $|\Delta\epsilon_{max}|r$ numbers were calculated from the $|\Delta\epsilon_{max}|$ data presented in Fig. 6a and mean particle radii derived from Table 1. Feedstock applied: ~20 μg ml^{-1} sonicated calf thymus DNA in 0.8 *M* potassium acetate, 10 m*M* EDTA, pH 5.5 buffer (conductivity of 59 mS cm^{-1}). 1—UFC ''20–40'' no ligand (ϵ_i=0.80); 2—Streamline DEAE (ϵ_i=0.77); 3—Streamline QXL (ϵ_i=0.77); 7—UFC ''20–40'' DEAE (ϵ_i=0.76); 8—UFC ''20–40'' PEI 2000 (ϵ_i=0.75); 9—UFC ''20–40'' PEI 25 000 (ϵ_i=0.75); 10—UFC ''20–40'' PEI 50 000 (ϵ_i=0.77); 11—UFC ''20–40'' DEAE dextran (ϵ_i=0.80).

more important factor than surface charge in determining binding capacity, and a similar conclusion is also obtained with respect to sensitivity to contraction (Fig. 6b). A uniform distribution of charge throughout the agarose component of the expanded bed supports is assumed, but for some supports, i.e., those carrying functionalised dextran chains or PEI, this may or may not be valid depending on the size and shape of the polymers and precise methods employed during support derivatisation. For example, short flexible dextran chains (M_r 35 000–40 000) are employed in the construction of Streamline QXL [33]. Their relatively small size permits access to the pores of epoxy-activated agarose (size exclusion pore dimension of ~25 nm [34]). The dextran chains and agarose matrix to which they are attached are then functionalised with quaternary amino methyl (Q) groups by reacting with glycidyltrimethyl ammonium chloride at high temperature. Thus for Streamline QXL an essentially uniform distribution of both charge (and dextran chains) throughout the agarose gel is envisaged (Fig. 7, left-hand side). In contrast, the molecular mass of the dextran chains used in the fabrication of the DEAE dextran-linked ''20–40'' μm prototype was very much larger (M_r 450 000–550 000) and the supports were then derivatised with DEAE·Cl under comparatively mild conditions [35]. These factors, combined with the much lower proportion of reactive primary hydroxyl groups on long dextran chains compared to short ones, leads us to deduce the following regarding the make-up (see Fig. 7, right-hand side) of this particular support: (i) the charge distribution is not uniform; (ii) the dextran chains are concentrated at the exterior particle surface; and (iii) are only very weakly derivatised with DEAE compared to the underlying agarose matrix.

Molecular size is also likely to play a role for the PEI, since Horn [36] reported that the degree of penetration of PEI into porous cellulose media is strongly dependent on its molecular mass. The molecular masses of the branched PEIs used in the preparation of PEI 2000, PEI 25 000 and PEI 50 000 ''20–40'' μm prototypes were 2000, 25 000 and >50 000, respectively. PEI was coupled to epichlorohydrin-activated supports [35] in salt-free aqueous solution at a pH of ~11 (which is close to recognised point of zero charge, 10.8, of the molecule [36]). According to Bulmer [29] and Horn [36] under these conditions the hydrodynamic radius of a PEI molecule with M_r of 50 000 is between 80 and 90 nm. Thus, exclusion of the high M_r PEI species (and to a lesser extent the PEI with an M_r of 25 000) from much of the pore volume of the agarose is likely, whereas the M_r 2000 PEI is expected to gain access to most of it (Fig. 8).

Finally, the M_r and concentration of PEI employed in the coupling reaction (Fig. 8) affect the conformation that a given PEI molecule adopts when it is covalently attached to a surface. The physical size and shape of branched PEI is strongly dependent on both environment (ionic strength, pH) and M_r. In

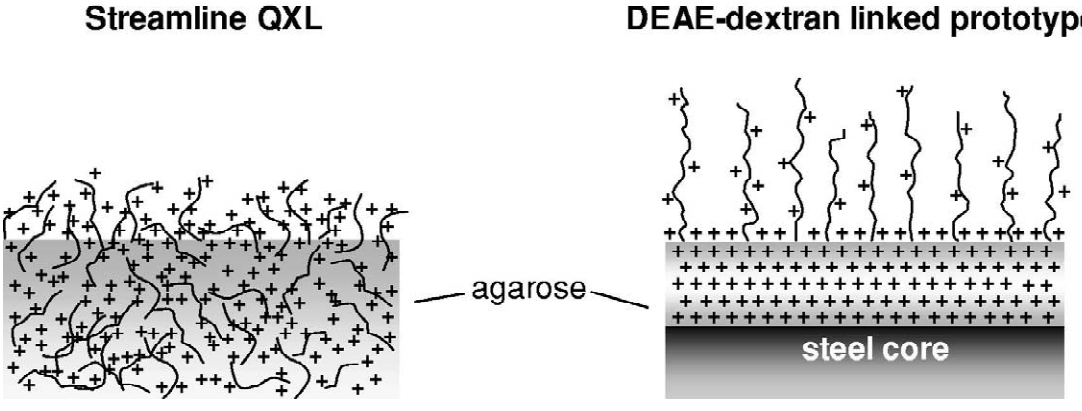

Fig. 7. Schematic illustration of the surfaces of Streamline QXL and DEAE–dextran-linked ''20–40'' μm prototype expanded bed adsorbents (see text for comments).

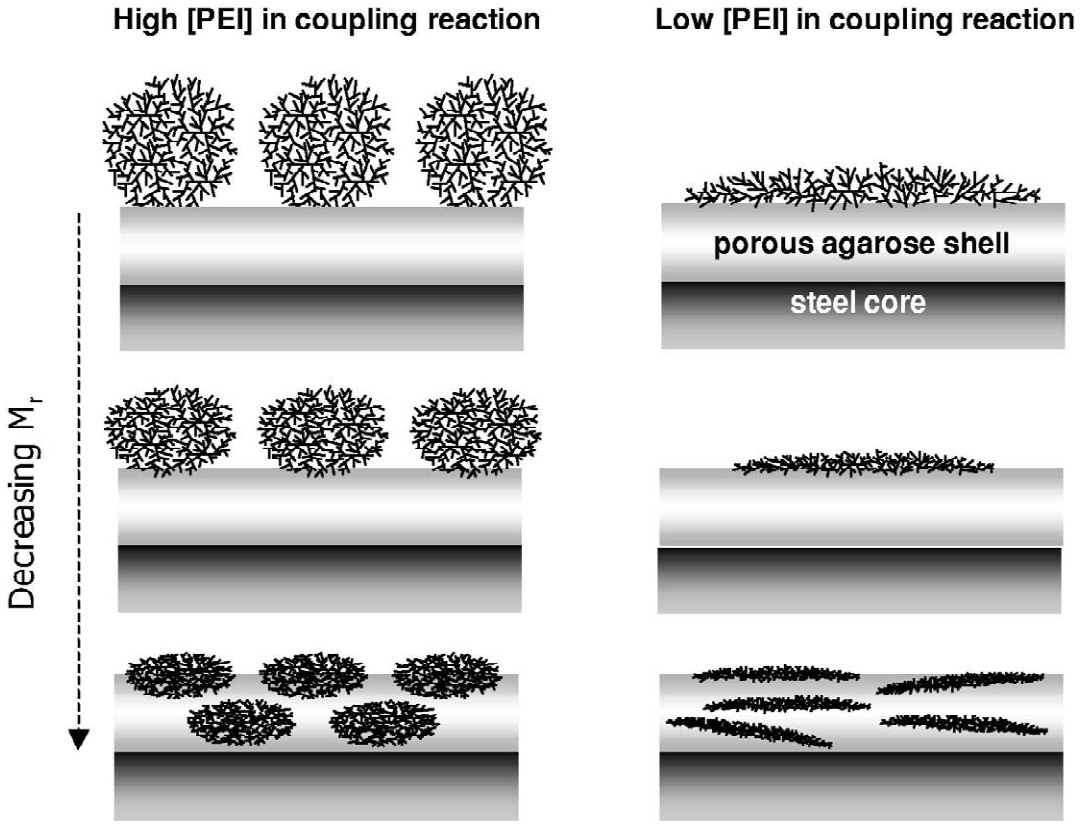

Fig. 8. Schematic illustration of the effect of PEI concentration in the coupling solution on the shape of immobilised PEI molecules and the distance they extend from the surface into the bulk phase.

free solution low M_r species have a flat disc-like shape, whereas larger molecules exist as coiled spheres. According to Horn [36] short polymers with high charge density tend to adsorb on surfaces in a flattened conformation, whereas larger molecules with fewer cationic charges adsorb via short polymer stretches or ''trains'' and the rest of the molecule extends away from the surface into the bulk phase in the form of ''loops'' and ''tails''. When coupling at high PEI concentrations (Fig. 8, left-hand side), as was done in the present case, the crowding at the surface forces the molecules to adsorb in an extended form, where covalent attachment to the surface is through a minimum number of sites. In contrast, when the PEI concentration is low (Fig. 8, right-hand side) the molecule is flattened against the surface via multi-site covalent interactions.

It is important to note that the differences in adsorbent appearance hypothesized above for supports bearing functionalised dextran chains (Fig. 7) or PEI (Fig. 8, left-hand side) are entirely consistent with the Q_r and $|\Delta\epsilon_{max}|r$ clustering patterns we have observed in Figs. 5b and 6b, respectively.

4. Conclusions

In this study we have examined the effects of particle size, charge density and polymeric surface ''extenders'' [33] on the dynamic binding capacity and bed dynamics during anion-exchange expanded bed adsorption of calf thymus DNA. We conclude that both binding capacity and sensitivity to bed contraction are clearly related to the external surface area afforded by porous expanded bed adsorbents,

i.e., capacity and contraction sensitivity with reduction in particle diameter.

Because of the very high charge density on DNA, it is surface area and not charge that is important in determining binding capacity. Thus, for DNA purifications, the use of weakly derivatised tentacle structures seems to be the best option as it enhances capacity without increasing sensitivity to inter-particle cross-linking. But whereas the DNA binding capacity is not strongly dependent on exposed surface charges, bed contraction most certainly is. The sensitivity of expanded beds of anion-exchange adsorbents is clearly related to the ability of a given particle surface to condense or compact DNA. Highly charged polymers are well known for their ability to condense nucleic acids [29,30] and PEI has in particular received considerable attention in recent years as a plasmid DNA compacting agent for use in non-viral gene therapy [37]. It is our opinion that the use of highly charged tentacle structures (especially large PEIs, but also shorter ones and Q-linked dextran chains) on surfaces of expanded bed beads should be avoided (especially when dealing with dirty heavily contaminated feedstocks) for both protein and nucleic acid separations.

For problem-free protein separations by anion-exchange EBA, especially with supports of small size, it is clear that radical re-design of expanded bed supports will be required in future. New breeds of expanded bed matrices should possess ''non-stick'' exteriors or barriers that are freely accessible to proteins, but not larger entities, such as long chain nucleic acids, cell debris fragments etc., and in order not to compromise to mass transport and sorption properties they must also be very thin.

Acknowledgements

I.T. gratefully acknowledges the financial support afforded by a Marie Curie Research Training Grant (No. ERB4001GT972611) and the Center for Process Biotechnology, BioCentrum-DTU.

References

[1] B.J. Spalding, Biotechnology 9 (1991) 229.
[2] A. Lyddiatt, D. O'Sullivan, Curr. Opin. Biotechnol. 9 (1998) 177.
[3] A.-K. Barnfield Frej, R.R. Hjorth, Ä. Hammarström, Biotechnol. Bioeng. 44 (1994) 922.
[4] H.A. Chase, Trends Biotechnol. 12 (1994) 296.
[5] J. Thömmes, in: T. Scheper (Ed.), Advances in Biochemical Engineering/Biotechnology, Vol. 58, Springer, Berlin, 1997, p. 185.
[6] F.B. Anspach, D. Curbelo, R. Hartmann, G. Garke, W.-D. Deckwer, J. Chromatogr. A 865 (1999) 129.
[7] J.J. Hubbuch, D.B. Matthiesen, T.J. Hobley, O.R.T. Thomas, Bioseparation 10 (2001) 99.
[8] J. Thömmes, A. Bader, M. Halfar, A. Karau, M.-R. Kula, J. Chromatogr. A 752 (1996) 111.
[9] R. Hjorth, Trends Biotechnol. 15 (1997) 230.
[10] Y. Kazumasa, N. Munehiro, O. Takao, S. Akinori, Eur. Pat. EP0699687 (1996).
[11] Amersham Biosciences, Downstream Magazine 28 (1999) 3.
[12] P.A. Munro, P. Dunnill, M.D. Lilly, Biotechnol. Bioeng. 19 (1977) 101.
[13] J.W. Eveleigh, J. Chromatogr. 159 (1978) 129.
[14] N. Ameskamp, C. Priesner, J. Lehmann, D. Lütkemeyer, Bioseparation 8 (1999) 169.
[15] J. Feuser, J. Walter, M.-R. Kula, J. Thömmes, Bioseparation 8 (1999) 99.
[16] J. Feuser, M. Halfar, D. Lütkemeyer, N. Ameskamp, M.-R. Kula, J. Thömmes, Process Biochem. 34 (1999) 159.
[17] H.M. Fernández-Lahore, R. Kleef, M.-R. Kula, J. Thömmes, Biotechnol. Bioeng. 64 (1999) 484.
[18] I. Theodossiou, M.A. Olander, M. Søndergaard, O.R.T. Thomas, Biotechnol. Lett. 22 (2000) 1929.
[19] I. Theodossiou, M. Søndergaard, O.R.T. Thomas, Bioseparation 10 (2001) 31.
[20] I. Theodossiou, Ph.D. Thesis, Technical University of Denmark, Lyngby, 2002.
[21] M.A. Olander, A.O.F. Lihme, T.J. Hobley, M. Simón, I. Theodossiou, O.R.T. Thomas, Int. Pat. Appl. WO 00/57982 (2000).
[22] I. Theodossiou, H.D. Elsner, O.R.T. Thomas, T.J. Hobley, J. Chromatogr. A 964 (2002) 77.
[23] R.C. Weast, Handbook of Chemistry and Physics, 70th edition, CRC Press, Boca Raton, 1989.
[24] J.M. Coulson, J.F. Richardson, J.R. Backhurst, J.H. Harker, Chemical Engineering, Vol.2, Pergamon Press, Oxford, 1991.
[25] I.D. Pitfield, Ph.D. Thesis, University of Cambridge, Cambridge, 1992.
[26] S. Roe, in: E.L.V. Harris, S. Angal (Eds.), Protein Purification Methods: A Practical Approach, IRL Press, Oxford, 1989, p. 200.
[27] A.I. Vogel, Vogel's Textbook of Quantitative Chemical Analysis, Bath Press, Avon, 1989.
[28] E. Zafirakos, A.O.F. Lihme, Bioseparation 8 (1999) 85.
[29] M. Bulmer, Ph.D. Thesis, University College London, London, 1992.
[30] D.E. Salt, S. Hay, O.R.T. Thomas, M. Hoare, P. Dunnill, Enzyme Microb. Technol. 17 (1995) 107.
[31] A. Ljunglöf, P. Bergvall, R. Bhikhabhai, R. Hjorth, J. Chromatogr. A 844 (1999) 129.

[32] R. Hammer, personal communication.
[33] H. Berg, H. Hansson and L. Kaagedal, International patent application WO9833572 (1998).
[34] L. Hagel, M. Östberg, T. Andersson, J. Chromatogr. A 743 (1996) 33.
[35] A.O.F. Lihme, personal communication.
[36] D. Horn, in: E.J. Goethals (Ed.), Polymeric Amines and Ammonium Salts, Pergamon Press, Oxford, 1980, p. 333.
[37] W.T. Godbey, K.K. Wu, A.G. Mikos, J. Controlled Release 60 (1999) 149.